Glassiness and constrained dynamics of a short-range nondisordered spin model

Juan P. Garrahan[1] and M. E. J. Newman[2]
[1]*Theoretical Physics, University of Oxford, 1 Keble Road, Oxford OX1 3NP, United Kingdom*
[2]*Santa Fe Institute, 1399 Hyde Park Road, Santa Fe, New Mexico 87501*
(Received 25 July 2000)

We study the low temperature dynamics of a two-dimensional short-range spin system with uniform ferromagnetic interactions, which displays glassiness at low temperatures despite the absence of disorder or frustration. The model has a dual description in terms of free defects subject to dynamical constraints, and is an explicit realization of the ''hierarchically constrained dynamics'' scenario for glassy systems. We give a number of exact results for the statics of the model, and study in detail the dynamical behavior of one-time and two-time quantities. We also consider the role played by the configurational entropy, which can be computed exactly, in the relation between fluctuations and response.

PACS number(s): 64.70.Pf, 75.10.Hk, 05.70.Ln

I. INTRODUCTION

Understanding the nature of the low-temperature dynamics of glasses and other strongly interacting many-body systems remains one of the outstanding open problems in condensed matter and statistical physics [1,2].

Consider, for example, the case of glass-forming supercooled liquids. One of the reasons for glassiness in such systems is that the rearrangements of atoms necessary for their relaxation involves activation over energy barriers. It is natural to plot the logarithm of the viscosity or equilibration time against the inverse temperature, giving a so-called Arrhenius plot, which should take a straight-line form if the barrier heights remain constant with varying temperature. For ''strong'' liquids [1], such as SiO_2, the Arrhenius plot is indeed a straight line, but for ''fragile'' liquids it is not, following instead the empirical Vogel-Fulcher law $\exp[\text{const}/(T-T_0)]$, although other forms not displaying a finite T singularity can be fit too [3]. If the dynamics of fragile liquids is due to activation (which is not the only possible explanation), this implies that the energy barriers grow with decreasing temperature, presumably because they increase with the increasing size of correlated regions in the system.

Another set of interesting questions, most relevant for fragile liquids, revolves around the possible existence of an ideal (continuous) phase transition to a true thermodynamic glass state at some temperature T_K (the Kauzmann temperature) lying below the glass temperature [4,5]. Although the existence of such a transition would resolve Kauzmann's paradox, in which the extrapolation of the configurational entropy of the supercooled liquid appears to pass below that of the crystal [6], and is also supported by the analogy between fragile glasses and discontinuous mean field spin glasses [7], there is some evidence against it. For example, it has been shown numerically [8] that a thermodynamic phase transition is absent for a system of polydisperse hard disks, a typical model glass former. It has also been argued that the extrapolations that yield a positive T_K in fragile liquids composed of molecules of finite size are flawed [9].

Given the many interesting open questions in this field, it is important to find simple and if possible solvable models for the various features displayed by glasses. The discontinuous mean-field spin glasses, such as the spherical p-spin model [10], provide a good example of such a model system. However, while some dynamical features of these models [2,11] are also observed in simulations of Lennard-Jones glasses [12,13], the presence of disorder in the models and, crucially, of long-range interactions limits their usefulness as models of systems that are intrinsically short-ranged and disorder-free, such as hard spheres in two and three dimensions.

An alternative approach to modeling these latter systems is the ''hierarchically constrained dynamics'' of Palmer *et al.* [14], in which it is hypothesized that, for a strongly interacting system displaying glassy behavior, it should be possible to describe the dynamics in terms of hierarchies of degrees of freedom, from fast to slow, independent of the presence of disorder or even frustration. These hierarchies would be weakly interacting in the energetic sense, but their dynamics would be constrained, the faster modes constraining the slower ones. It is known that the presence of kinetic constraints in the dynamics can directly induce glassiness. A good example is the kinetically constrained Ising chain [15–17], for which the Hamiltonian is trivial, but the transition rates for the flipping of individual Ising spins depend on the states of neighboring spins. Kinetic constraints can also arise as a result of entropic barriers, as in the Backgammon model, for instance [18]. Fragile glass behavior has also been observed in kinetic lattice-gas models [19,20]. Although interesting in their own right, these models have somewhat *ad hoc* dynamics, and represent only one side of the scenario discussed in Ref. [14]. A recent comparative study of one-dimensional constrained kinetic models has been given by Crisanti *et al.* [21].

In this paper, we study in detail a model introduced by Newman and Moore [22], which is a form of two-dimensional Ising model with uniform short-range ferromagnetic interactions. Despite the absence of either disorder or frustration, this model displays glassy behavior at low temperatures. The cause of this behavior is the presence of energy barriers that grow logarithmically with the size of correlated regions. The model has a dual description in terms either of strongly interacting spins subject to simple single-

spin-flip dynamics, or of free ''defects'' subject to a constrained dynamics. It is thus an explicit realization of the constrained dynamics scenario of Palmer *et al.* [14]. Other nondisordered short-range spin systems displaying glassy features are three-dimensional Ising models with competing nearest and next-nearest neighbor interactions [23], or with ferromagnetic four-spin plaquette interactions [24–26].

The paper is organized as follows. In Sec. II, we describe the model and extend the exact solution of the statics given in Ref. [22] by calculating all equilibrium spin-correlation functions, and showing that the phase transition to an ordered state occurs only at zero temperature. In Sec. III, we give our principal results, which concern the out-of-equilibrium dynamics of the system following a quench from a random configuration to low temperatures. We show that the equilibration time diverges with an exponential inverse temperature squared law, similar to that found for the asymmetrically constrained Ising chain. We study the behavior of one-time quantities, such as energy density and spin correlations and two-time quantities, such as autocorrelation and response functions. We also study the out-of-equilibrium fluctuation-dissipation relations and relate them to the configurational entropy, which can be calculated exactly. Our conclusions are given in Sec. IV.

II. MODEL AND STATIC SOLUTION

We consider the model introduced in Ref. [22], which consists of Ising spins $\sigma=\pm 1$ on a triangular lattice with uniform short-range three-spin ferromagnetic interactions: each spin interacts only with its nearest neighbors, and only in groups of three lying at the vertices of a downward-pointing triangle on the lattice. Note that this is distinct from the model of Baxter and Wu [27], which has interactions on upward-pointing triangles also (and which is not glassy). The Hamiltonian for the model is

$$H=\frac{1}{2}J\sum_{mn}\ \sigma_{mn}\sigma_{m,n+1}\sigma_{m-1,n+1}+\frac{1}{2}NJ, \tag{1}$$

where the indices m and n run along the unit vectors of the lattice $\vec{a}_1\equiv\hat{x}$ and $\vec{a}_2\equiv\frac{1}{2}(\hat{x}+\sqrt{3}\hat{y})$. The constant in the Hamiltonian is added for convenience to make the minimum possible energy equal to zero. The model can also be formulated using the defect variables

$$\tau_{mn}\equiv\sigma_{mn}\sigma_{m,n+1}\sigma_{m-1,n+1}, \tag{2}$$

in terms of which the Hamiltonian is

$$H=\frac{1}{2}J\sum_{mn}\ \tau_{mn}+\frac{1}{2}NJ. \tag{3}$$

On lattices of the size of a power of two in at least one direction, with periodic boundary conditions, there is a one-to-one correspondence between spin and defect configurations, and hence the partition function is given by

$$Z=\left(2e^{-(1/2)\beta}\cosh\frac{1}{2}\beta\right)^{N}, \tag{4}$$

where N is the number of spins, and we set $J=1$ from here on. The equilibrium energy density is then

$$\varepsilon_{\mathrm{eq}}=\frac{1}{2}(1+\langle\tau\rangle)=\frac{1}{2}\left(1-\tanh\frac{1}{2}\beta\right). \tag{5}$$

We now wish to invert Eq. (2) and write the spins as functions of the defects. It is known [22] that if the spins are represented by the variables $s_{mn}\equiv\frac{1}{2}(\sigma_{mn}+1)\in\{0,1\}$, the spins below an isolated defect on the lattice form a Pascal's triangle mod 2 [i.e., a triangular array with the binomial coefficients $\binom{n}{r}$ mod 2 as entries]. This means that the value of the spin s_{mn} is given by the superposition mod 2 of the Pascal's triangles of all defects $\tau_{kl}=+1$ with $m-l\leqslant k\leqslant m$ and $l\geqslant n$. The inverse of the transformation (2) then reads

$$\sigma_{mn}=-\prod_{\substack{n\leqslant l\\ m-l\leqslant k\leqslant m}}(-\tau_{kl})^{\binom{l-n}{m-k}}. \tag{6}$$

With this result we can compute the equilibrium correlation functions of the spins. First, the magnetization is given by averaging Eq. (6):

$$\langle\sigma_{mn}\rangle=-\left(\tanh\frac{1}{2}\beta\right)^{\mathcal{N}_{mn}}, \tag{7}$$

where

$$\mathcal{N}_{mn}=\sum_{\substack{n\leqslant l\\ m-l\leqslant k\leqslant m}}\binom{l-n}{m-k}\ \mathrm{mod}\ 2 \tag{8}$$

is the total number of ones in the inverted Pascal's triangle with its tip at site (m,n). This number diverges faster than the linear size of the triangle, so in the thermodynamic limit we obtain

$$\langle\sigma_{mn}\rangle=\begin{cases}-1 & \text{for } T=0\\ 0 & \text{for } T>0,\end{cases} \tag{9}$$

for all (m,n), implying that the system has a $T=0$ static phase transition.

Arbitrary correlation functions can be computed in a similar manner:

$$\langle\sigma_{mn}\cdots\sigma_{m'n'}\rangle=-\left(\tanh\frac{1}{2}\beta\right)^{\mathcal{N}_{mn\cdots m'n'}}, \tag{10}$$

where now $\mathcal{N}_{mn\cdots m'n'}$ is the total number of ones in the superposition mod 2 of the inverted Pascal's triangles starting in positions (m,n) through (m',n'). Since $\binom{l}{0}=\binom{l}{l}=1$, the left and right edges of a Pascal's triangle contain only ones, so any superposition of two triangles always has an infinite number of ones coming from the edges. This implies that *all* two-spin correlations vanish at $T>0$. The first nonzero correlations are those for three spins at the vertices of inverted equilateral triangles of side 2^k. In this case $\mathcal{N}=3^k$, and the correlation is

$$C_k^{(3)}=\langle\sigma_{mn}\sigma_{m,n+2^k}\sigma_{m-2^k,n+2^k}\rangle=-\left(\tanh\frac{1}{2}\beta\right)^{3^k}. \tag{11}$$

Notice that

$$C^{(3)}_{k+1}\left(\tanh\frac{1}{2}\beta\right)=C^{(3)}_{k}\left(\tanh^3\frac{1}{2}\beta\right). \tag{12}$$

A similar scaling relation is seen in the one-dimensional Ising model.

At low temperatures the system is in a scaling region, and using Eq. (11) we find a correlation length of

$$\xi=\left(\ln\coth\frac{1}{2}\beta\right)^{-\ln 2/\ln 3}. \tag{13}$$

III. DYNAMICS

Newman and Moore [22] found that the model studied here shows glassy behavior under a single-spin-flip dynamics. They showed that following a quench from $T=\infty$, the system was unable to equilibrate in finite time at a low enough temperature ($T\lesssim 0.2$ for $t_{\max}\sim 10^9$ in their simulations). The system also fell out of equilibrium for exponential cooling with a variety of cooling rates. The reason for this glassiness is to be found in the details of the system's dynamics. Single-spin flips correspond to flips of the defect variables on triples of sites forming upward-pointing triangles on the lattice, and sets of such flips can be combined to flip upward-pointing triangles of side 2^k for any integer k. Any isolated such triangle with $k>0$ is locally stable; in order to remove it we have to cross an energy barrier of height k. Thus, as the system relaxes it has to cross energy barriers that grow logarithmically with the size of the equilibrated regions.

Another way of looking at this is to observe that at low temperatures the flipping of an isolated defect is heavily suppressed, since such a flip requires the creation of two other defects and so incurs a net energy penalty. Thus, a defect requires the presence of another neighboring defect to be able to flip, a situation highly reminiscent of the facilitated kinetic Ising model of Ref. [15]; the defects are noninteracting in the Hamiltonian, but their low temperature dynamics is effectively constrained.

At low temperatures, excitations of linear size larger than one can only be annihilated via activation. From the observation that barriers grow logarithmically with linear size, it is straightforward to estimate equilibration time. The rate of relaxation of an excitation of linear size d is given by the Arrhenius formula $\Gamma(d)\sim\exp(-\ln d/T\ln 2)$. Thus after time t, the average linear distance between defects is $d\sim t^{T\ln 2}$. The equilibrium value of this distance at low T is $d_{\rm eq}\sim\exp(\beta/2)$ [see Eq. (5)], and hence the equilibration time is

$$t_{\rm eq}\sim\exp\left(\frac{1}{2\,T^2\ln 2}\right). \tag{14}$$

This exponential inverse temperature squared (EITS) form is similar to that obtained in Ref. [17] for the asymmetrically constrained Ising chain (ACIC) [16], except for the 2 in the denominator that is due to the two-dimensional nature of our model. The EITS form has no finite-temperature singularity, which is consistent with the fact that our model has no finite-temperature phase transition. The behavior of the relaxation, however, is ''fragile.'' In fact, the EITS form can be approximated by a Vogel-Fulcher form with $T_0\sim\frac{2}{3}T_g$. A system that has an analogous but ''strong'' behavior is the Frenkel-Kontorova model [28]: at low temperatures above its $T=0$ phase transition, the relaxation of defects is hindered by the presence of constant energy barriers, and the equilibration time diverges in an Arrhenius way.

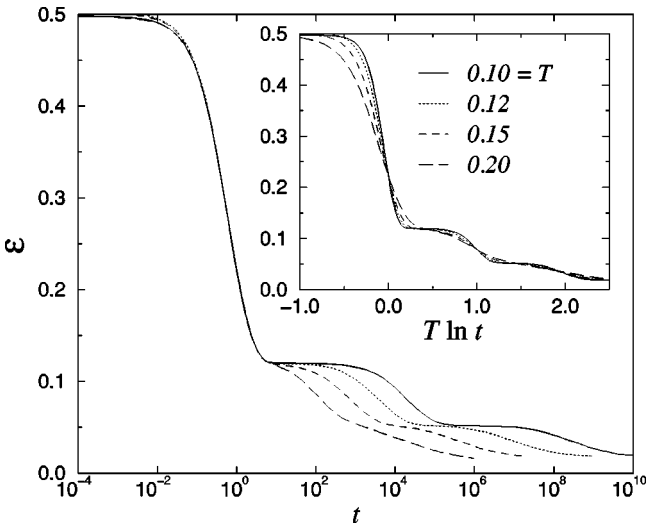

FIG. 1. Energy density $\varepsilon=\langle H\rangle/N$ as a function of time following a quench from $T=\infty$ to $T=0.10$, 0.12, 0.15, and 0.20, from Monte Carlo simulations for a system of 256×256 spins. Time is in Monte Carlo steps per spin, and all magnitudes are in dimensionless units. Inset: the same data as a function of rescaled time $\nu=T\ln t$.

Equation (14) clarifies the observations made in Ref. [22]. In the case of relaxation following a quench from $T_0=\infty$ to T, the highest temperature at which the system was found to equilibrate within time $t_{\max}=10^9$ was $T=0.2$, while for $T=0.18$ or smaller, the system was unable to reach equilibrium. This is explained by the fact that $t_{\rm eq}(T=0.2)\sim 10^8$, while $t_{\rm eq}(T=0.18)\sim 10^{10}$. In the case of exponential cooling, our expression for $t_{\rm eq}$ implies a maximum allowable cooling rate of $\gamma_{\max}(T)\sim 1/t_{\rm eq}(T)$ if we wish to remain in equilibrium at temperatures T and greater. For the different annealing simulations of [22], the temperatures at which the energy ceases to follow the equilibrium curve are given by the solution of $\gamma_{\max}(T)=\gamma$ for the cooling rate γ used.

A. One-time quantities

We now consider the behavior of one-time quantities for the model, such as energy density and spin correlations, following a quench from $T=\infty$ to a low temperature.

The $T=\infty$ configuration is random, and therefore has zero correlation length. As the system relaxes following the quench, it tries to increase its correlation length to the equilibrium value, Eq. (13), which is finite but large at low temperature. In terms of the defects, the system is trying to decrease the defect density or equivalently the internal energy per spin ε from its initial value of $\varepsilon_0=\frac{1}{2}$. In Fig. 1, we show numerical results for the evolution in time of the energy density after a quench from $T=\infty$ to a variety of final temperatures. The simulations were performed on a 256×256 rhombic lattice using a Bortz-Kalos-Lebowitz continuous time algorithm [29]. As the figure shows, after an initial

temperature-independent exponential relaxation corresponding to the (barrierless) removal of pairs of neighboring defects, the energy displays ''plateaus,'' which are more pronounced the lower the temperature. These plateaus are the result of the system becoming trapped in locally stable configurations. As we can see, the time taken by the system to escape these plateaus becomes larger with decreasing temperature.

As shown in the previous section, the typical length scale in the system (i.e., the typical distance separating defects) grows with time as t^T, and in the absence of other length scales, we might thus expect the data in Fig. 1 approximately to collapse when plotted against t^T, or equivalently against $\nu = T \ln t$ on the logarithmic scales used in the figure. (A collapse of this kind was found for the ACIC in Ref. [17].) In the inset of Fig. 1, we show that this is indeed the case for our model. Save for the initial exponential transient, the collapse of the curves for different temperatures is very good. Moreover, the first plateau seems to extend from $\nu = 0$ to 1, the second from $\nu = 1$ to 2, and so on (a behavior also seen in the ACIC).

At low temperatures, the relaxation of the system can also be regarded as an anomalous coarsening process. For the case considered here of periodic boundary conditions, there exists a unique minimum energy configuration of the model in which all the spins point down and there are no defects. For free boundary conditions, however, there are 2^{2L-1} degenerate minima. (The spins along the bottom and right-hand side of our rhombic system, for instance, may be chosen arbitrarily, with the rest being uniquely fixed by the requirement that there be no defects.) Following a quench, spins start to rearrange locally to eliminate defects, regardless of the boundary conditions, and thus form domains of the various free-boundary minima. The imperfect matching of these domains will be marked by the presence of defects.

The coarsening dynamics for T close to zero can be studied approximately using the generating function method of Sollich and Evans [17]. Consider a description of a configuration of the system in terms of domains containing no defects ($\tau = -1$) bounded by sites containing defects ($\tau = 1$). In contrast with the one-dimensional model studied in [17], such a description cannot be made exact for our model. Nevertheless, as far as average properties go, such as distance between defects, we can think of low-energy configurations as an approximate tiling of defect-free parallelograms each delimited by a defect in, say, its top right-hand corner. This effectively maps the problem into one dimension. As we now show, this crude approximation, which allows us to apply the method of Ref. [17], gives reasonable results.

When $T \to 0$, we have $\varepsilon_{\rm eq} \to 0$ and the plateaus of Fig. 1 become distinct stages in the dynamics. During stage n, all domains of linear size d in the interval $2^{k-1} < d \leq 2^k$ are annealed away. The time scale for this process is $O(e^{\beta k})$, and differs by a factor of e^{β} from the time scale associated with the following stage. In this limit, the master equation for the coarsening process can be solved using generating functions. If $P_k(d)$ is the probability distribution of lengths d at the beginning of the kth stage, $G_k(z) = \Sigma_{2^{k-1} < d} P_k(d) z^d$ is the probability generating function for this distribution, and $H_k(z) \equiv \Sigma_{2^{k-1} < d \leq 2^k} P_k(d) z^d$ is the equivalent function for the active domains—those which will be annealed away during the current stage—the following recursive relations are obtained [17]:

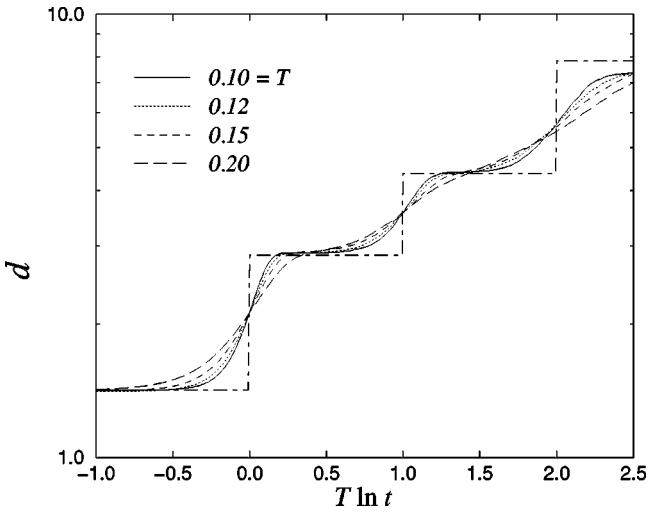

FIG. 2. Average distance between defects d as a function of rescaled time $\nu = T\ln(t)$. The dotted-dashed line corresponds to the $T = 0$ coarsening approximation.

$$G_{k+1}(z) = 1 + [G_k(z) - 1] \exp[H_k(z)]. \tag{15}$$

Given an initial distribution $P_0(d)$, these equations can be solved numerically.

In Fig. 2, we show the average linear length of the domains $d(t) = 1/\sqrt{\varepsilon(t)}$ as a function of $\nu = T \ln t$ from our simulations. As $T \to 0$, we expect $d(t)$ to become a ''staircase'' function, with the steps extending between integer values of ν. The approximate heights of these steps are given by the derivative of the generating function at $z = 1$: $\langle d \rangle_k = \Sigma_d d P_k(d) = G_k'(1)$. These steps are also plotted in the figure (dotted-dashed line) and, as we can see, the agreement is quite good.

We now turn to the behavior of the spin correlation functions as we approach equilibrium. In equilibrium, as shown above, the magnetization and all two-spin correlations vanish at any finite temperature. Moreover, at all times following a quench, the average magnetization and all equal-time two-spin correlations vanish as well, as shown in Fig. 3. This is a consequence of the three-spin interactions: regardless of the value of a spin i, the Hamiltonian favors a neighboring spin j equally to be up or down, since the only interaction between the two spins also includes a third spin of unknown orientation.

In equilibrium, the first nonzero correlations are those for triplets of spins at the vertices of downward pointing triangles of linear size 2^k. This is also the case in the out-of-equilibrium regime following a quench. In Fig. 4, we show the absolute value of the three-spin correlations $|C_k^{(3)}|$ as a function of time after a quench, for various values of k. The behavior of these curves illustrates the nature of the stages by which relaxation takes place. Initially, correlations at all length scales are zero. The system has no barriers to relaxation of excitations of length scale 1, so $|C_0^{(3)}|$ starts to grow immediately after the quench. At $\nu = T \ln t = 0$, $|C_1^{(3)}|$ grows exponentially fast to a first quasistationary value, while all $C_{k>1}^{(3)}$ remain zero: this first plateau corresponds to partial

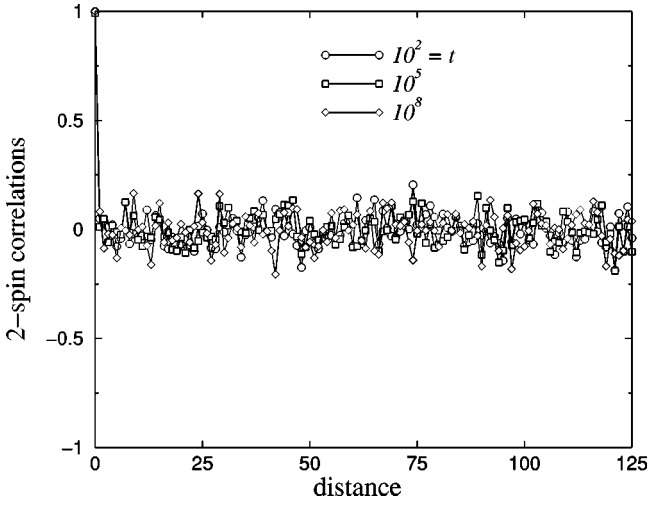

FIG. 3. Two-spin correlations for various times as a function of distance.

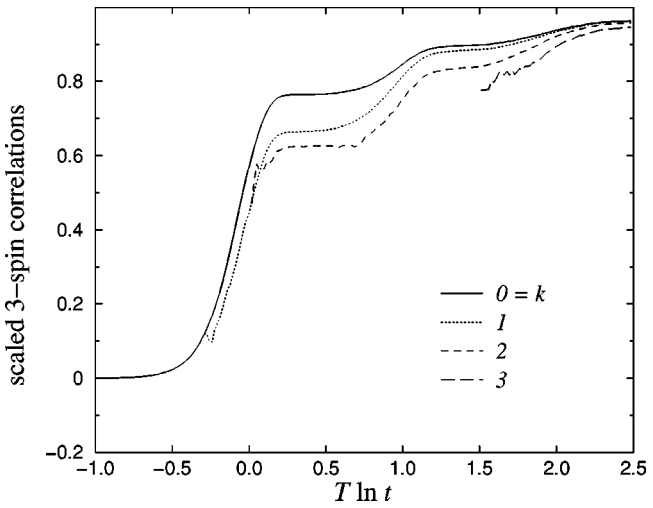

FIG. 5. Three-spin correlations scaled according to Eq. (12).

equilibration up to length scales of 2. At $\nu=1$, the system starts to relax up to length scales of 4, with $C_2^{(3)}$ becoming nonzero, while $C_{k>2}^{(3)}=0$. And so forth.

Within the plateaus all one-time quantities have roughly stationary values, and so it is natural to ask to what extent the system is in a quasiequilibrium state. One answer to this question comes from examining the agreement between our nonequilibrium correlation functions and the exact relations (12) for the equilibrium correlation function. In Fig. 5, we compare $|C_0^{(3)}|$ with $|C_k^{(3)}|^{(1/3^k)}$, and find that the out-of-equilibrium correlation functions still collapse approximately when scaled appropriately, the collapse getting better as time progresses. This may indicate that the later stages can be described by an approximate equilibrium at an appropriate effective temperature. We discuss this point further in Sec. III C.

B. Two-time quantities

We now turn to the behavior of two-time quantities in the out-of-equilibrium regime following a quench from high temperature. We first consider the local two-time spin autocorrelation function

$$C(t,t_w)=\frac{1}{N}\sum_{mn}\langle\sigma_{mn}(t)\sigma_{mn}(t_w)\rangle. \tag{16}$$

In Fig. 6, we show $C(t,t_w)$ for quenches from $T=\infty$ to $T=0.12$ for three different values of the weighting time t_w, as a function of the rescaled time difference $\nu=T\ln\tau$, with $\tau=t-t_w$. The three values of t_w used correspond to $\nu=0$, 1, 2, i.e., to the starting points of the first three of the plateaus discussed in Sec. III A. In Fig. 7, we present the same correlations as a function of t/t_w.

Since the system does not reach equilibrium at $T=0.12$ on the time scales simulated, we do not in general expect the correlation functions to be functions of the time difference $\tau=t-t_w$ only. In fact, as Fig. 6 shows, the behavior of the correlation functions has a clear dependence on the waiting time. On the other hand, as we can see from Fig. 7, neither does it obey a simple aging form, scaling with t/t_w, as ob-

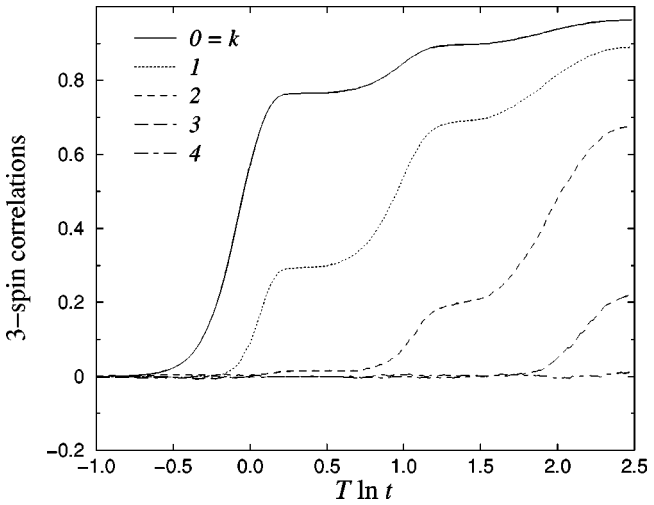

FIG. 4. Three-spin correlation functions $C_k^{(3)}$ as a function of time, for linear sizes $2^{k=0,1,2,3,4}$. We plot the absolute value of the correlations.

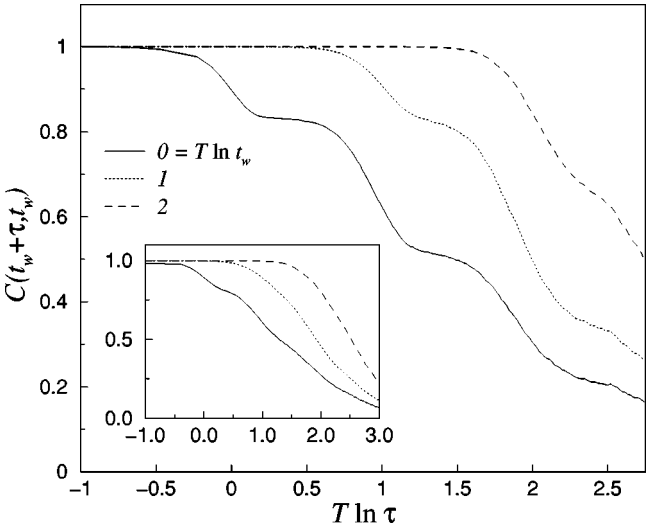

FIG. 6. Local spin-spin correlation functions as a function of the scaled time difference $T\ln\tau$, following a quench to $T=0.12$. Inset: the same for $T=0.20$.

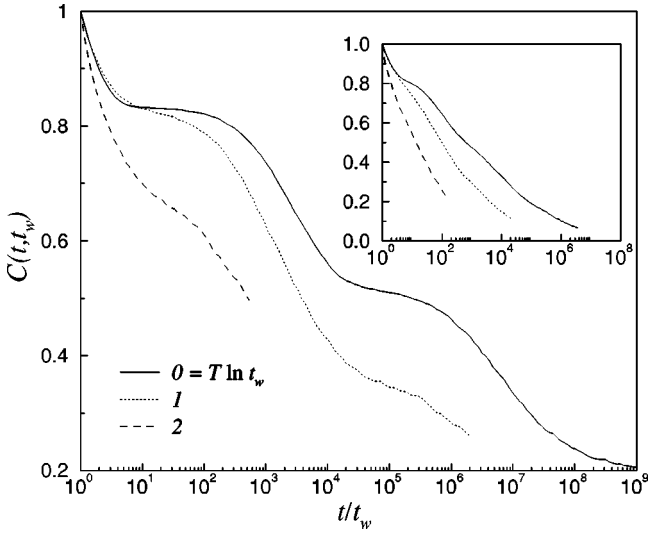

FIG. 7. Local spin-spin correlation functions as a function of t/t_w, for $T=0.12$. Inset: the same for $T=0.20$.

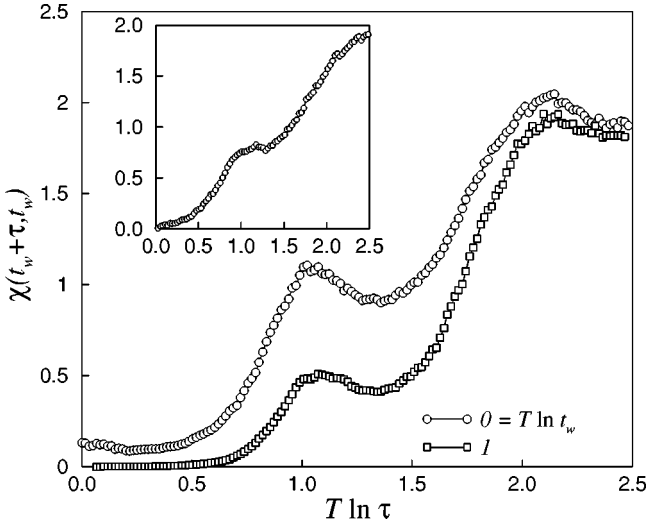

FIG. 8. Integrated response function vs rescaled time difference, for $T=0.12$ and $T\ln t_w=0$ and 1. Inset: the same for $T=0.20$.

served in other cases [2]. This is because the length scale associated with the relaxation of the spins does not grow as a simple power of time (see Figs. 2 and 4). In general, if equilibration is associated with the growth of a length scale $l(t)$, then the two-time correlation functions should scale with $l(t)/l(t_w)$ [2]. Behavior of this kind was found in the autocorrelation functions for the ACIC [21], where the appropriate length scale is the average distance between upward-pointing spins. In our model, however, rescaling the spin correlation functions by the distance between defects fails, and we have not been able to find a suitable length scale such that the scaling with $l(t)/l(t_w)$ holds.

Another observable of interest is the response function $\chi(t,t_w)$, which measures the response of the spins at time t to a small field applied at time t_w. Comparison of such a response function with the two-time correlations studied above can reveal violations of the fluctuation-dissipation theorem (FDT) that are expected in systems displaying aging. In general, in order to obtain the response function corresponding to the *local* correlation function calculated above, we would need to apply a field to only a single spin on the lattice, or equivalently we could apply a random field and measure the staggered response [30]. Both of these approaches present significant numerical challenges, and require a substantial investment of CPU time in simulation to extract clean results. For our model, however, this turns out to be unnecessary because, as mentioned in Sec. III A, all off-diagonal spin-spin correlations vanish, implying that two-time autocorrelations of the magnetization $m\equiv N^{-1}\Sigma_{mn}\sigma_{mn}$ are proportional to the local spin correlations thus:

$$\langle m(t)m(t')\rangle=\frac{1}{N}C(t,t'). \tag{17}$$

This means that we need only to measure the response to a uniform field.

We have performed simulations in which the Hamiltonian was perturbed with a small uniform magnetic field applied at a time t_w following a quench to finite temperature: $\Delta H(t)=h_0\theta(t-t_w)\Sigma_{mn}\sigma_{mn}$. We measured the integrated response (or relaxation function)

$$\chi(t,t_w)=\frac{1}{Nh_0}\sum_{nm}\langle\sigma_{nm}(t)\rangle_h, \tag{18}$$

which is equivalent to measuring the change in magnetization per spin of the system, divided by the strength of the applied field. We have experimented with a variety of different values for the field strength h_0; the results presented here are for $h_0=0.02$, which we find to be well within the linear regime. In Fig. 8, we show the measured response for $T=0.12$ and $\nu_w=T\ln t_w=0$ and 1. Notice that the response is not in general a monotonically increasing function of time, but instead shows cusps at times corresponding to the jumps between plateaus. For higher temperatures the cusps are less pronounced and eventually disappear (see inset).

A similar nonmonotone behavior is seen in the response function for the defects in our model, and can be understood physically by the following argument. The energy density ε plays a role for the defects equivalent to that played for the spins by the magnetization m, and the equivalent of a small applied magnetic field δh is a small change in temperature $\delta T=-T^2\delta h$. Consider then the behavior of the energy density shown in Fig. 1. At low temperatures, we expect ε to follow a staircase function, with steps extending between integer values of ν. When the field is applied (i.e., when the temperature is changed), the perturbed energy density is another staircase function, with each step having a slightly higher (lower) value for the negative (positive) field, and lasting a longer (shorter) time, the steps now extending between integer values of $\nu(1-T\,\delta h)$. The corresponding integrated response is given by the difference between the perturbed and unperturbed energy densities, divided by the field. Within each plateau this difference is mostly small and roughly constant, but a sharp change is seen at the boundaries between steps. The unperturbed $(T\to 0)$ density jumps

to the next plateau when ν is an integer, but the perturbed one only does so when $\nu(1-T\,\delta h)$ is an integer, and thus the absolute value of the response is large during the short interval between these two events. Once the perturbed density jumps to the next plateau, the response becomes small again. This increase and decrease at integer ν is responsible for the humps seen in the integrated response. The argument generalizes to perturbations with a staggered random field.

The response function for the ACIC was studied in Ref. [21], where it was found to be a monotonically increasing function of time. However, as mentioned above, the defect representation of our model behaves very similarly to the ACIC, and we therefore conjecture that nonmonotone behavior will be seen in the ACIC also at sufficient low temperatures, for precisely the reasons given above.

C. Configurational entropy and fluctuation-dissipation relations

A configuration of our model is a local energy minimum if and only if no two defects occupy adjacent sites on the lattice. In the context of glasses, such states are known as inherent structures [31]. A nice feature of the model is that the set of inherent structures is isomorphic to the set of allowed states of Baxter's hard-hexagon model [32], allowing the distribution of inherent structures to be calculated exactly.

The grand-partition function of the hard-hexagon model on a lattice of N sites is

$$Z_N(z)=\sum_{M=0}^{N} g(M,N)z^M, \tag{19}$$

where z is the fugacity and $g(M,N)$ is the number of ways of placing M nonadjacent particles on the triangular lattice. In our case, $M=N\varepsilon$ corresponds to the total energy of our model, so $g_N(\varepsilon)\equiv g(N\varepsilon,N)$ gives the density of states for inherent structures with energy ε. For large N, $g(n,N)$ is exponential in N, so that $g_N(\varepsilon)=e^{NS_c(\varepsilon)}$, where $S_c(\varepsilon)$ is the configurational entropy of the model, i.e., the entropy density of metastable states. In this case, Eq. (12) becomes

$$Z_N(z)=\int d\varepsilon\, \exp[N\{\varepsilon \ln z+S_c(\varepsilon)\}]. \tag{20}$$

For large N, the integral is dominated by the saddle point in the exponent, and we obtain

$$\varepsilon(z)=\frac{\partial \ln \kappa}{\partial \ln z}, \tag{21}$$

$$S_c[\varepsilon(z)]=\ln \kappa(z)-\varepsilon(z)\ln z, \tag{22}$$

where $\kappa(z)\equiv \lim_{N\to\infty}[Z_N(z)]^{1/N}$ is the partition function per site of the hard-hexagon model, which is known exactly in the thermodynamic limit [32]. Between them, Eqs. (19) and (21) determine $S_c(\varepsilon)$ parametrically.

At low defect densities, $S_c(\varepsilon)$ reduces to

$$S_c(\varepsilon)=-\varepsilon \ln \varepsilon+O(\varepsilon), \tag{23}$$

which is the general form for a low concentration of noninteracting point defects in an ordered structure [9]. The configurational entropies of the disordered Ising chain, constrained Ising chains, and the Backgammon model all have this asymptotic form [21,33]. Note that S_c has infinite slope with respect to ε at $\varepsilon=0$ where it vanishes, which is consistent with the fact that none of these models has a finite temperature phase transition. However, since S_c' increases logarithmically as ε is decreased, an extrapolation of $S_c'(0)$ from the behavior at finite ε would wrongly suggest a finite slope and therefore a finite Kauzmann temperature. It has been argued that this mechanism would rule out an ideal-glass phase transition in materials composed of limited size molecules and conventional molecular interactions [9].

Having calculated correlation and response functions for the spins in our model (Sec. III B), we can use our results to study the relation between fluctuations and responses, which in some other systems is related to the configurational entropy. The natural way to do this is by means of a parametric plot of $\chi(t_w+\tau,t_w)$ vs $C(t_w+\tau,t_w)$ for fixed t_w [11]. For a system in equilibrium at temperature T, such a plot would be linear with slope $-1/T$, in accordance with the fluctuation-dissipation theorem. In a glassy system on the other hand, the FDT is normally violated in the out-of-equilibrium low-temperature regime as $t_w\to\infty$, and this violation encodes important information about the system's dynamical behavior (see Ref. [2] for a review). The classic example is the mean-field p-spin spin glass [10], for which the FDT plot is piecewise linear: for large values of C, corresponding to relaxation of fast degrees of freedom, the plot has a slope of $-1/T$ as it would in equilibrium, but for smaller C, corresponding to the relaxation of slow modes, it has slope $-1/T_{\rm eff}$, where $T_{\rm eff}>T$ is interpreted as a effective temperature for these modes [34]. Furthermore, in the p-spin model, $T_{\rm eff}$ is numerically equal to the inverse of the slope of the configurational entropy at the asymptotic energy density [35]. Similar behavior has also been observed in more realistic model glass formers [12,13].

At sufficiently low temperatures our model is clearly out of equilibrium, and although it does not reach the long-time asymptotic regime corresponding to approach to equilibrium in our simulations, it is possible that the FDT plots can still provide information on the relaxation process, and maybe that there exist effective temperatures associated with the different time scales in the problem [34]. In Fig. 9, we show the FDT plot for the spin response and correlation functions. The unusual nonmonotonic shape is a consequence of the nonmonotonicity of the response function.

The curves should be ''read'' from right to left in the plot, and are composed of a sequence of segments, each associated with one of the plateaus. The starting point of each segment and the part of the curve in which the response is increasing correspond to the time the system spends within the relevant plateau. The maximum and the downward portion of the segment correspond to the transition to the next plateau. The first part of each segment has a shape similar to that found in Refs. [36] and [37] for the one-dimensional Ising model following a quench into the temperature scaling region: the FDT curve there has slope $-1/T$ at $C=1$, and

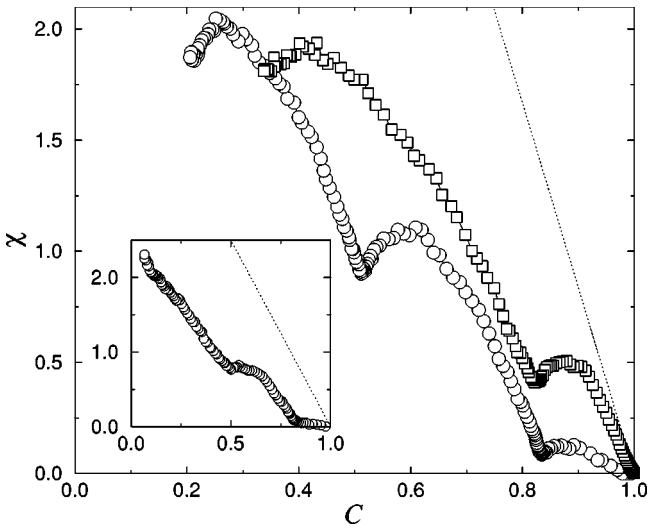

FIG. 9. Parametric plot of integrated response vs the two-time autocorrelation function of the spins for $T=0.12$ and $T \ln t_w=0$ and 1. The dotted line corresponds to slope $-1/T$. In the inset, we show the same for $T=0.20$ and $T \ln t_w=0$.

bends continuously with decreasing C to reach a slope of $-1/2T$ at $C=0$. (Note that this behavior is very different from that seen in domain growth in higher dimensions [30].) In our model, each of the segments of the FDT plot starts with slope approximately $-1/T$ (indicated by the dotted line in the figure), but the subsequent shape of the curve varies from one segment to another. The similarity within the plateaus to the behavior of the one-dimensional Ising model is consistent with what was found for the statics of the model in Sec. II.

An important open question is whether the configurational entropy of Eqs. (21) and (22) plays any role in the out-of-equilibrium dynamics. A plausible explanation for the shape of the FDT curves of Fig. 9 is that the initial part of each segment corresponds to quasi-stationary thermal excitations of fast modes, while the latter part corresponds to slower large-scale rearrangements arising from occasional jumps between local minima before the transition to the next plateau takes place. If the slope of the latter part of each segment corresponds to an effective temperature for that segment, we might expect these temperatures to be related to the rate of change of $S_c(\varepsilon)$ at the energy density of the associated plateau. It is noteworthy that the final slopes of each segment in Fig. 9 are roughly equal to $1/S_c'(\varepsilon_k)$, with values approximately $\frac{1}{2}$, $\frac{1}{3}$, and $\frac{1}{4}$ for the first three plateaus. This observation is however, speculative and furthermore contrasts with the conclusions of Ref. [21] for the ACIC, so it deserves further investigation.

IV. CONCLUSIONS

In this paper, we have studied the low-temperature behavior of the glassy two-dimensional spin model with uniform ferromagnetic short-range three-spin interactions introduced by Newman and Moore. The model has a dual description in terms either of interacting spins or of free defects, the mapping between the spin and defect representations being one-to-one. This allows us to compute exactly all equilibrium correlation functions, both for spins and defects. We have also shown that the model displays no static phase transition at finite temperature.

Despite the simplicity of its statics, the model's low-temperature single-spin-flip dynamics is highly nontrivial. A spin flip in the model corresponds to the flipping of three neighboring defects, which implies that at low temperatures the dynamics of the defects is constrained: a defect can only be flipped if another neighboring defect is present. This in turn implies that the relaxation of isolated defects is an activated process, and the size of the corresponding energy barriers are found to grow logarithmically with the distance between defects. The dual representation of the model in terms of strongly interacting spins with a simple dynamics, and of free defects subject to kinetic constraints, is an explicit realization of the hierarchical constrained dynamics scenario of Palmer *et al.* [14].

We have studied in detail the dynamics of the model after a quench to low temperatures. The presence of logarithmically growing barriers leads to non-Arrhenius relaxation, the equilibration time being of the exponential inverse temperature squared form $t_{\rm eq} \sim \exp(1/[2T^2 \ln 2])$. One-time quantities such as internal energy display ''plateaus'' in their equilibration profiles, which correspond to the trapping of the system in local energy minima. Each plateau is associated with a specific stage in the dynamics, the kth plateau corresponding to the partial equilibration of length scales up to 2^k. The behavior of observables related to the defects is strikingly similar to that seen in the asymmetrically constrained Ising chain. For example, in the $T \to 0$ limit, the average distance between defects can be well approximated using the analytic methods of Sollich and Evans [17] that yield exact results for the asymmetrically constrained model.

We have also studied two-time quantities for the model, such as spin autocorrelations and response functions. At low temperatures, the response functions have the unusual property of being nonmonotonic: they display humps at exactly those times at which the system jumps between plateaus. This behavior has also been observed in other models at times well within the activated regime, such as the constrained Ising chains and the Backgammon model in one dimension [21], models for two-dimensional froths [38], and vibrated granular media [39]. An important open question is whether this is a generic feature of the out-of-equilibrium dynamics of activated processes.

ACKNOWLEDGMENTS

The authors would like to thank Jean-Philippe Bouchaud, Paul Goldbart, Jorge Kurchan, Felix Ritort, David Sherrington, and Peter Sollich for useful discussions. J.P.G. wishes to thank the Santa Fe Institute and MEJN, the Subdepartment of Theoretical Physics, University of Oxford, for their kind hospitality while this work was carried out. This work was funded in part through EC Grant No. ARG/B7-3011/94/27 and EPSRC Grant No. GR/M04426.

[1] C.A. Angell, Science **267**, 1924 (1995).
[2] J.-P. Bouchaud, L. F. Cugliandolo, J. Kurchan, and M. Mézard, in *Spin-Glasses and Random Fields*, edited by A. P. Young (World Scientific, Singapore, 1997).
[3] C. A. Angell, P. H. Poole, and J. Shao, Nuovo Cimento D **16**, 993 (1994).
[4] J.H. Gibbs and E.A. Di Marzio, J. Chem. Phys. **28**, 373 (1958); G. Adam and J.H. Gibbs, *ibid.* **43**, 139 (1965).
[5] J. Jäckle, Rep. Prog. Phys. **49**, 171 (1986).
[6] W. Kauzmann, Chem. Rev. **43**, 219 (1948).
[7] T.R. Kirkpatrick and D. Thirumalai, Phys. Rev. Lett. **58**, 2091 (1987); T.R. Kirkpatrick and P. Wolynes, Phys. Rev. B **36**, 8552 (1987).
[8] L. Santen and W. Krauth, Nature (London) **405**, 550 (2000).
[9] F.H. Stillinger, J. Chem. Phys. **88**, 7818 (1988).
[10] A. Crisanti and H.-J. Sommers, Z. Phys. B: Condens. Matter **87**, 341 (1992).
[11] L.F. Cugliandolo and J. Kurchan, Phys. Rev. Lett. **71**, 173 (1993).
[12] W. Kob and J.-L. Barrat, Phys. Rev. Lett. **78**, 4581 (1997).
[13] R. Di Leonardo, L. Angelani, G. Parisi, and G. Ruocco, Phys. Rev. Lett. **84**, 6054 (2000).
[14] R.G. Palmer, D.L. Stein, E. Abraham, and P.W. Anderson, Phys. Rev. Lett. **53**, 958 (1984).
[15] G.H. Fredrickson and H.C. Andersen, Phys. Rev. Lett. **53**, 1244 (1984).
[16] J. Jäckle and S. Eisinger, Z. Phys. B: Condens. Matter **84**, 115 (1991).
[17] P. Sollich and M.R. Evans, Phys. Rev. Lett. **83**, 3238 (1999).
[18] F. Ritort, Phys. Rev. Lett. **75**, 1190 (1995).
[19] J. Kurchan, L. Peliti, and M. Sellito, Europhys. Lett. **39**, 365 (1997).
[20] M. Sellito, J. Phys.: Condens. Matter **12**, 6477 (2000).
[21] A. Crisanti, F. Ritort, A. Rocco, and M. Sellitto, e-print cond-mat/0006045.
[22] M.E.J. Newman and C. Moore, Phys. Rev. E **60**, 5068 (1999).
[23] J.D. Shore, M. Holzer, and J.P. Sethna, Phys. Rev. B **46**, 11 376 (1992).
[24] A. Lipowski, J. Phys. A **30**, 7365 (1997).
[25] A. Lipowski, D. Johnston, and D. Espriu, Phys. Rev. E **62**, 3404 (2000).
[26] M.R. Swift, H. Bokil, R.D.M. Travasso, and A.J. Bray, e-print cond-mat/0003384.
[27] R.J. Baxter and F.Y. Wu, Phys. Rev. Lett. **31**, 1294 (1973).
[28] S.L. Shumway and J.P. Sethna, Phys. Rev. Lett. **67**, 995 (1991).
[29] A.B. Bortz, M.H. Kalos, and J.L. Lebowitz, J. Comp. Physiol. **17**, 10 (1975).
[30] A. Barrat, Phys. Rev. E **57**, 3629 (1998).
[31] F.H. Stillinger and T.A. Weber, Phys. Rev. A **25**, 978 (1982).
[32] R.J. Baxter, *Exactly Solved Models in Statistical Mechanics*, (Academic Press, London, 1982).
[33] G. Biroli and R. Monasson, Europhys. Lett. **50**, 155 (2000).
[34] L.F. Cugliandolo, J. Kurchan, and L. Peliti, Phys. Rev. E **55**, 3898 (1997).
[35] R. Monasson, Phys. Rev. Lett. **75**, 2847 (1995).
[36] C. Godreche and J.M. Luck, J. Phys. A **33**, 1151 (2000).
[37] E. Lippiello and M. Zannetti, Phys. Rev. E **61**, 3369 (2000).
[38] L. Davison and D. Sherrington, e-print cond-mat/0008039.
[39] M. Nicodemi, Phys. Rev. Lett. **82**, 3734 (1999).